ARTICLE

Improved and Large Area Single-Walled Carbon Nanotube Forest Growth by Controlling the Gas Flow Direction

Satoshi Yasuda,[†] Don N. Futaba,[†] Takeo Yamada,[†] Junichi Satou,[†] Akiyoshi Shibuya,[‡] Hirokazu Takai,[‡] Kouhei Arakawa,[‡] Motoo Yumura,[†] and Kenji Hata[†,§,*]

[†]Nanotube Research Center, National Institute of Advanced Industrial Science and Technology (AIST), 1-1-1 Higashi, Tsukuba 305-8565, Japan, [‡]ZEON Corporation, 1-6-2 Marunouchi, Chiyoda-ku, Tokyo 100-8246, Japan, and [§]Japan Science and Technology Agency (JST), Kawaguchi, 332-0012, Japan

ABSTRACT A gas shower system was introduced to improve the growth of single-walled carbon nanotube (SWNT) forests by controling the gas flow direction. Delivery of gases from the top of the forest enabled direct and precise supply of ethylene and water vapor to the Fe catalysts. As such, this approach solved one of the limiting factors of water-assisted chemical vapor deposition method (CVD), that is, delivery of the very small optimum water level to the catalysts. Consequently, this approach improved SWNT forests growth stability, uniformity, reproducibility, carbon efficiency (32%), and catalyst lifetime. With this improved growth, we could synthesize a 1 cm tall forest with 1 × 1 cm size. Also we employed this approach to grow an A4 size SWNT forest to highlight the scalability of water-assisted CVD.

KEYWORDS: carbon nanotube · forest · water-assisted chemical vapor deposition · gas delivery · lifetime

When single-walled and multi-walled carbon nanotubes are efficiently grown by chemical vapor deposition (CVD) from catalysts deposited on a substrate, the subsequently grown nanotubes align vertically into a bulk material called a SWNT forest[1−7] and MWNT forest,[7−16] respectively. CNTs within the forest possess excellent properties, such as, alignment, high surface area, high carbon purity, good electrical conductivity, and long length. As such, possessing these important properties, CNT forests have been shown to be advantageous for numerous applications spanning a wide range of fields, exemplified from three-dimensional MEMS,[17] stretchable conductors,[18] high power and density supercapacitors,[19] sensing applications,[20] field-emitters in flat-screen displays,[21] superhydrophobic surfaces for self-cleaning surfaces,[22] fast-moving, low-voltage actuators,[23] super-tough fibers,[24] gecko tape,[25] and fuel cells.[26]

From these pioneering researches, the potential applications of CNT forests have been revealed, however their use in real applications has been precluded so far mainly because production of forests have been limited. Therefore, to pursue and utilize the full promise of CNT forests, the development of a synthetic approach that enables efficient, large-area, economical, and stable growth of CNT forests is of paramount importance. Such a synthetic approach, if realized, might advance the use of CNT forests toward commercial applications. In the past, many synthetic approaches have been proposed to address the above-mentioned issues, including, but not limited to, HiPco process,[27] alcohol CVD,[1] plasma CVD,[6,11] and "flying carpets".[16] A different approach introduced a small amount of water into the growth ambient of standard chemical vapor deposition (CVD)[2,3,7,19,21] to increase the growth rate and lifetime of the catalysts, and thus dramatically improve the synthesis efficiency of SWNTs[2,19,21] and MWNTs[3,7] to unprecedented heights. Specifically, with an almost background level of (100−200 ppm) water, SWNTs and MWNTs could grow into millimeter scale forests within 10 min. Water acted to remove the carbon coating on the catalyst to revive catalyst activity for high synthesis efficiency.[28] This water-assisted highly efficient growth, denoted as "supergrowth," has become a popular method to efficiently grow forests; however, the application of only a minute amount of water to the catalysts on the substrate (base growth mechanism) had seriously hindered the controllability, reproducibility, and stability. Research of precise and controlled gas delivery for CVD has a long history, and for CNT forest growth, use of patterned catalysts has been proposed to introduce a gas channel for fast and efficient mass transfer.[29] Another different direction is to use a shower head to dispense gases for better control of growth.[30,31]

*Address correspondence to Kenji-hata@aist.go.jp.

Received for review July 3, 2009 and accepted November 19, 2009.

Published online November 30, 2009.
10.1021/nn9007302

This technique is widely used in the semiconductor industry because precise and uniform growth over large areas is required.

In this article, we utilized this gas shower system to deliver water vapor and carbon source gas from the top of the forests, rather than from the side. By this delivery method, water vapor and carbon source gas flowed parallel to the CNTs within the forest, and were directly delivered to the catalysts with minimal loss. This facilitated precise, uniform, and direct delivery of a minute amount of water to the catalysts on the substrate and consequently improved the growth significantly. The improvements of this approach address most aspects of growth including long lifetime, increased growth yield, height, carbon efficiency, and scalability for large area growth, and additionally improved stability and reproducibility. As such, we believe that this approach would serve as one key to enable industrial-scale mass production of economical CNTs.

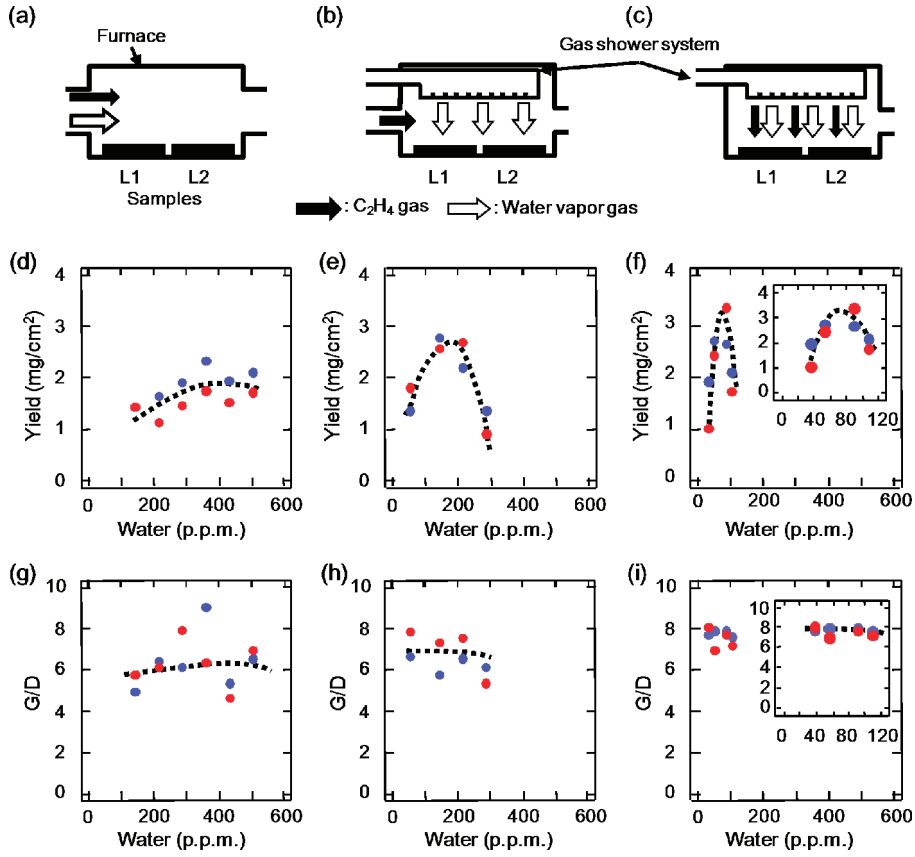

Figure 1. Schematics of (a−c) three different gas delivery methods and plots of (d−f) the SWNT forest yield and (g−i) G/D ratio at 10 min growth as a function of the water level for L1 and L2 samples. (a) Conventional lateral-flow growth where all gas flows from the side, (b) water top-flow growth where only water vapor gas flows from the gas shower, and (c) top-flow growth where water vapor and carbon source gases are delivered from the gas shower. SWNT yield and G/D ratio for (d and g) conventional lateral-flow, (e and f) water top-flow, and (f and i) top-flow growths, respectively. Red and blue circles indicate the L1 and L2 samples, respectively.

Figure 1 panels a−c schematically show the concept of the shower system to deliver water vapor and carbon source gas from the top compared to conventional lateral-flow growth where the gas flows in from the side and out the other. Specifically, a 60 × 20 mm quartz shower system with a 27 array of 0.5 mm holes (see Supporting Information, Figure S1) was installed in a 1 in. quartz lateral tube furnace (Supporting Information, Figure S2) and placed above and parallel to the sample (Figure 1c). As shown in the schematics, three types of growths and sample configuration (L1 and L2) with different gas deliveries were implemented on these samples: (i) water vapor and carbon source gas (ethylene) both incident from the side (conventional *lateral-flow* growth), (ii) only water vapor from the top (*water top-flow* growth), and (iii) both water vapor and carbon source gas (ethylene) from the top (*top-flow* growth), with different water levels.

The growth yield, particularly the sensitivity to water, and the graphitic (G-band) to disorder band (D-band) ratio measured by Raman (532 nm wavelength) spectroscopy showed significant dependence on the gas delivery. The three cases showed similar overall trends, that is, the growth yield increased, peaked, and decreased with the water level, but with markedly different sensitivities (Figure 1d−f). The lateral-flow growth and the top-flow growth represented the two extremes in all cases. While conventional lateral-flow growth showed relatively the weakest sensitivity to water as evident in the indistinct and broad peak (Figure 1d), the top-flow growth was significantly more water sensitive as reflected in the sharp and narrow peak (Figure 1f). The sensitivity of the water top-flow growth fell between the two extremes (Figure 1e). In similar fashion, for the water level required to optimize the growth and the resultant growth yield, the top-flow growth required the smaller level than that of the other cases while possessing the highest growth yield at the optimized condition. Meanwhile, the lateral-flow growth required the highest optimized water level yet producing, relatively, the lowest yield. Once more, the water top-flow growth fell between the two in both categories. In contrast to the growth properties, the quality of the nanotubes did not appear to depend on the gas delivery as the G/D ratio was similar for all three cases (Figure 1g−i). Another important aspect of the shower was its ability to improve growth stability, uniformity, and reproducibility and to facilitate growth on larger areas. For the top-flow growth, the difference between two simultaneously grown samples L1 and L2 (Figure 1f,i) and fluctua-

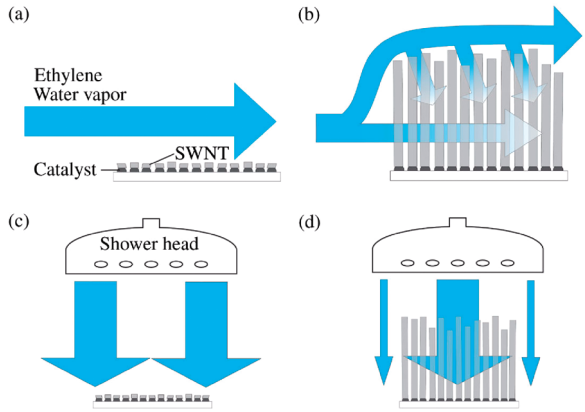

Figure 2. Schematics of gas flow direction to catalysts at initial stage of the growth and with the presence of a forest for (a and b) conventional lateral-flow and (c and d) top-flow growth, respectively.

tion between successive growths were small in terms of the yield and G/D ratio. In contrast, conventional lateral-flow growth showed a large difference between the L1 and L2 samples (Figure 1d,g) and strong fluctuation among growths (Table 1). We believe this instability reflects the difficulty in controlling the supergrowth. Furthermore, the yields of 10 consecutive growths for the three types of gas delivery (see Supporting Information, Figure S3) showed that the top-flow growth demonstrated the best reproducibility (fluctuation among growths) and uniformity (fluctuation between samples), and the highest yield. It should be noted that the catalyst was not a critical factor in this work, and we could apply the top-flow growth to synthesize SWNT, DWNT, or MWNT forests by tailoring the catalyst thicknesses.[7]

These results clearly show that the top-flow growth was valuable to control and regulate the growth of forests. In addition, not only did top-flow growth produce the highest yield, this method exhibited an exceptionally high carbon efficiency (the percentage of the input carbon converted to CNTs) of 32% which is over an order higher than the 1% carbon efficiency from the lateral-flow growth (Table 1).

We interpret that the difference in the growth with different gas delivery originates from stable and uniform delivery of water vapor and carbon source gas to the catalyst (Figure 2). The forest mass densities were calculated by dividing the weight by volume and as 0.03−0.04 g/cm.[3,32] As calculated from the mass density, the average distance between SWNTs (average size 2.8−3.0 nm) was ~14 nm. Ethylene and water vapor transfer through the forest by Knudsen diffusion because the mean free paths of ethylene and water vapor calculated as 405 and 180 nm, respectively, are an order larger than the mean distance between SWNTs in the forest.[29] This means that a forest acts as a diffusion barrier to water and ethylene similar to a nanoporous layer.

TABLE 1. Summary of the Yield and G/D for L1 and L2 Samples for Each Growth Process Synthesized by 10 Continuous Growths

process	yield[a] (CV[b])	G/D (CV[b])	RD[c] of yield	RD[c] of G/D	carbon efficiency
lateral-flow	2.0 ± 0.5(0.25)	6.2 ± 0.8(0.13)	−38%	−3%	0.9%
water top-flow	2.3 ± 0.3(0.13)	7.8 ± 0.4(0.05)	−13%	+3%	1.1%
top-flow	3.4 ± 0.4(0.12)	6.8 ± 0.6(0.09)	−6%	−3%	32%

[a]Unit of yield is mg/cm^2. [b]CV is coefficient of variation. [c]RD is relative difference between L1 and L2 samples.

For conventional lateral-flow growth, at the initial stage of the growth, the gases diffuse over the substrate by ordinary molecular diffusion (Figure 2a), and this allows a uniform and optimum supply of the gases to the catalysts. In contrast, under the presence of a forest, gases that contact the forest would feel a diffusion barrier and thus a part would pass across the top by molecular diffusion. Consequently, a part of the gases would penetrate into the forest from the side and from the top, transport through the nanoporous forest by Knudsen diffusion, and reach the catalyst at the root (Figure 2b). As the forest develops with time, the amount and ratio of ethylene and water vapor supplied to the catalysts would not only vary spatially and but also temporally, making it impractical to supply the optimum levels of gases to the catalysts over a large area for extended time. In addition, it should be remembered that the optimum required water level is extremely small on the hundreds of ppm level and that water could react and be consumed by the quartz tube or any carbon impurities on the tube before they reach the forest, which would affect the growth stability and sensitivity. In fact, Fourier transform infrared (FT-IR) spectroscopy detected CO in the exhaust gases providing direct evidence of reaction of water and carbon during the growth process. These observations mean that the water level reaching the catalyst varies spatially and deviates from the water level supplied to the forest, and this explains the observed broad and high water level window associated with lower yield for the lateral-flow growth.

In contrast, for top-flow growth, the shower head forces the gases to flow into the forest with minimum flow around the forest (Figure 2c), and this facilitates a uniform and optimum supply of the gases to the catalysts. In addition, the gases diffuse parallel to the CNT alignment direction and encounter minimal interruption, and thereby reach the catalysts by the shortest possible path with minimum diffusion barrier. As such, even with the presence of the forest, the flow is expected to be rather unvarying (Figure 2d). These effects explain the observed sensitivity, stability, uniformity, high carbon efficiency, and high yield of the top-flow growth.

We found that the top-flow possessed an additional benefit of increasing the catalyst lifetime that enabled the synthesis of centimeter tall CNT forests. To illustrate this point, three forest growth curves (Figure 3a) using the three different gas deliveries were measured by the *in situ* telecentric height monitoring system (LS7030M, Keyence).[33] In brief, a brilliant parallel green light was transmitted into the furnace and the

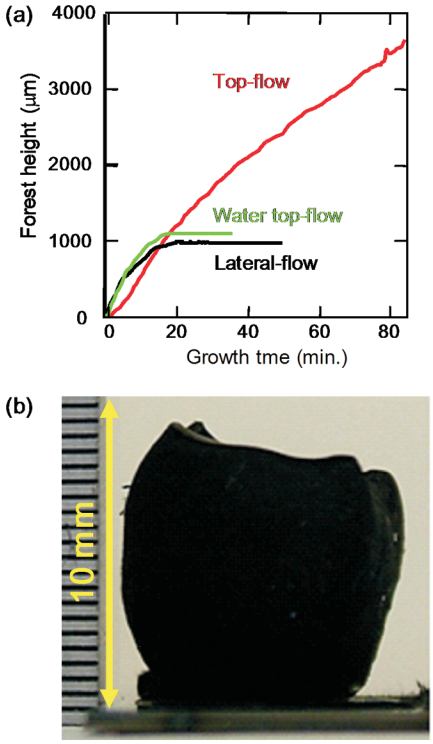

Figure 3. (a) Time evolution of the forest growth observed *in situ* telecentric optical monitoring system for the three different growths. (b) Photograph of CNT forest with a height of 1 cm synthesized by top-flow growth.

projected shadow of the forest progressed to the receiver and was refocused onto a CCD through a telecentric optical system. The growth curves of the lateral-flow and water top-flow growth were almost identical and followed the radioactive decay growth model as previously reported, that is, the growth rate was highest at the onset of growth, gradually decreased, and finally terminated.[34] A significant difference was observed for the top-flow growth. Although, the growth rate was initially slightly slower, the decrease in the growth rate was nominal over a long duration, and consequently, the forest kept growing. In fact, the top-flow growth curve was concaved up while the other growth curves were concaved down below 20 min. This means that the growth rate increased from the onset of the growth. We interpret that this unusual concaved growth behavior originates from the small total flow of gases (100 sccm) of the top-flow growth that is an order smaller than that of the lateral-flow growth (1000 sccm). Accordingly, at the onset of growth, the concentration of carbon at the catalysts does not immediately reach the critical value of supersaturation as is the case for lateral-flow growth. Instead, the concentration of the carbon gradually rises and CNTs precipitate from the catalyst when the critical value is exceeded. The growth accelerates as the carbon concentration builds up. This effect would result in a concaved down growth behavior as observed in this work and has been also reported in growth where a low level of carbon source was supplied by a molecular jet.[35]

By extending the growth time, we synthesized a 1 cm tall forest with 1 × 1 cm size (Figure 3b) while maintaining a ~50 μm/min average growth rate. In fact, the growth terminated when the forest reached the gas shower delivery system, and thus we expect that growing even taller forests is possible. For top-flow growth, the growth rate remained almost unchanged over a wide range, and almost no saturation in growth was observed in sharp difference with the other reports where a growth termination has been observed.[34,36,37] The observed long lifetime would provide an important evidence to understand the long debated mechanism of growth termination, and here we provide several possible explanations. First, it should be noted that the lifetime of growth strongly depends on the relative level of water to carbon source gas supplied to the catalysts. When catalysts are exposed to the optimum relative level of water to carbon (~1:2000), the surfaces are kept clean and active, and thus the lifetimes are long.[34] Deviation from the optimum level results in shorter lifetime from catalyst deactivation because excess water oxidizes the catalysts and excess carbon smothers the catalysts. As explained above, as the height of the forest increases, the ability to maintain the optimum levels at the catalysts decreases for lateral-flow growth. This effect could be one reason for the shorter lifetime of lateral-flow growth. Another explanation is the very high carbon efficiency of 32% of the top-flow growth. For typical low efficiency CNT synthesis (less than 10%), we believe that the unreacted carbon species contribute to the deactivation of surrounding catalyst particles. This effect results in the shorting of the growth lifetime. On the basis of this high carbon efficiency reported here, we interpret that the concentration of the unreacted carbon species would decrease significantly because upon contact with the catalyst ethylene effectively converted into CNTs. We tentatively interpret that this effect accounts for the observed long lifetime. Growth termination has been one of the main obstacles in CNT growth, and top-flow growth provides a simple yet effective approach to address to this issue.

We found that growths with different gas delivery produced almost identical SWNTs that demonstrate that gas delivery rules the growth kinetics but not the structure of the SWNTs. First, Raman spectra showed that the radial breathing mode peaks, an indicator of the existence of SWNTs, and the G/D ratio were almost identical for the three types of growths (Figure 4a). Second, transmission electron microscopy (TEM) images revealed that the diameter, straightness, and impurity levels of the SWNTs were similar for all the three types of growths (Figure 4b). The average sizes of the SWNTs were estimated to be in the range of 2.5 to 3 nm, and did not depend on the growth type. Third, thermogravimetric profiles (not shown) of the CNTs synthesized by the three types of

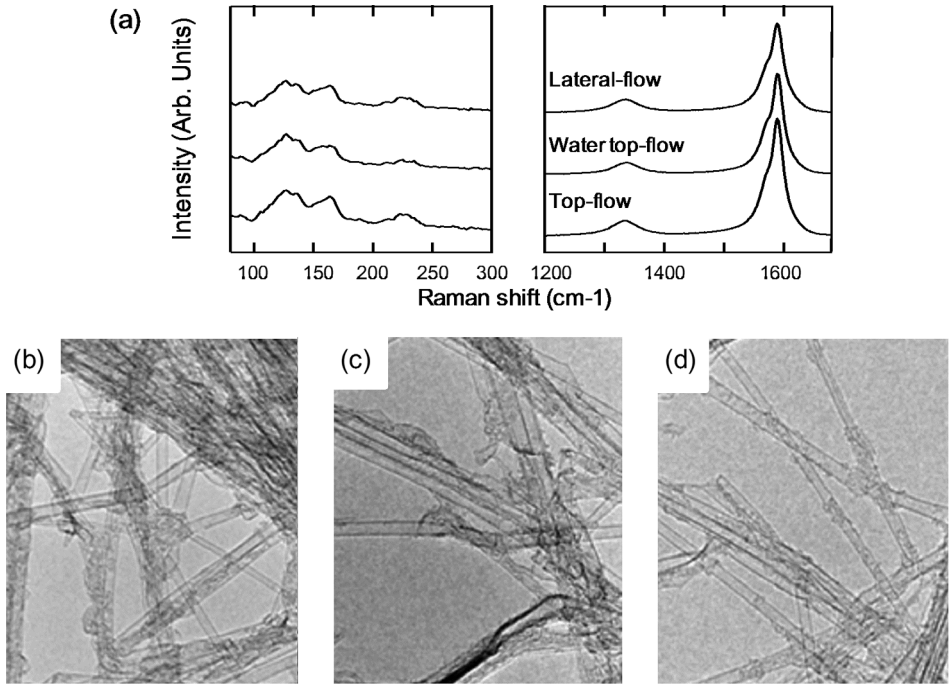

Figure 4. Charactarization of SWNT forests. (a) Raman spectra of SWNT forests grown by conventional lateral-flow, water top-flow, and top-flow growths. TEM images of SWNTs grown by (b) conventional lateral-flow, (c) water top-flow, and (d) top-flow growths, respectively.

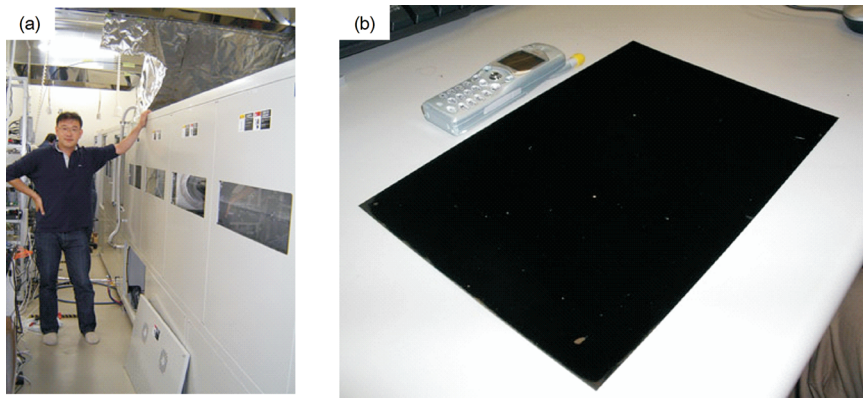

Figure 5. Photographs of (a) constructed 6 m × 1.5 m lateral batch CVD furnace and (b) grown A4.

growth were nearly identical with negligible weight reduction at low temperatures below 500 °C, followed by the main combustion in the range of 550−700 °C, and no measurable residue above 750 °C.

Finally, to demonstrate the potential of the top-flow growth to synthesize forests on large scale, we constructed a 6 × 1.5 m lateral batch CVD furnace that could accommodate a sample up to A4 size (210 mm × 297 mm). This furnace was equipped with a gas shower delivery system designed by thermofluid simulations to deliver the water uniformly across the entire substrate (Figure 5a). To ensure uniformity of the catalyst on this large sample, we used a large sputtering instrument with the capability to sputter and rotate a sample as large as 500 × 500 mm (see Supporting Information, Figure S4). The A4 samples were placed off-centered and rotated providing uniformity of thickness within 10%. This uniformity was sufficient to prepare a catalyst film appropriate to grow SWNTs (0.8−1.3 nm in thickness) across the entire A4 substrate.[3] With this large-area CVD furnace we could synthesize a forest covering all of the A4-size substrate with a height approaching a millimeter and weight exceeding a gram in a 10 min growth time (Figure 5b). This important result clearly demonstrates that the supergrowth process is scalable in two-dimension, and opens up a route for mass production of CNT forests based on this approach. Such a large area forest could be directly used as a large blackbody light absorber for solar energy collectors[38] or could be transformed into densely packed SWNT solid large sheets useful for electrodes of compact and high energy density supercapacitors.[19] In contrast, we failed to obtain a large area forest by lateral-flow growth because the water level reaching the catalyst at downstream side was smaller than that at the upstream side. When the water level supplied to the forest was tuned to the optimum level of the upstream/downstream side, we got inferior growth yield at the opposite downstream/upstream side. If the sample length was over 4 cm, we could not grow forests across the entire sample, and this highlights the superiority of top-flow growth for large-scale.

In conclusion, we demonstrated that the gas flow direction is a very important factor that governs many aspect of supergrowth. By delivering both carbon source gas and water vapor from the top, they could flow parallel to the CNT alignment, and thus reach the catalysts with high efficiency, stability, and uniformity. This approach improved not only the stability and reproducibility of growth but also the lifetime of the catalysts that resulted in an increase of yield and height. While conventional lateral-flow growth only possesses scalability in one dimension, this approach is fundamentally scalable in two dimensions as demonstrated by the successful growth of forests on A4 size substrates. Accordingly, this simple approach provides a powerful tool to unlock the full potential of supergrowth.

METHODS

Single-walled carbon nanotube forests were synthesized in a 1 in. quartz tube furnace by water-assisted chemical vapor deposition, "supergrowth" at 750 °C (referring to set temperature of the furnace) on two 2 × 2 cm Si wafer samples (L1 and L2) with Al_2O_3 10 nm/Fe 1 nm catalyst. The catalysts were prepared by a sputtering process. As the prepared Fe thin film was around 1.0 nm and very thin, it was preferred to have a sputtering rate that was as slow (but stable) as possible. To maximize our control over sputtering levels, we minimized the sputtering rate to deposit a 1.0-nm-thick Fe film with a time exceeding 30 s. This ensures that the deposition process is both very stable and uniform. Conventional lateral-flow growth were performed by introducing 100 standard cubic centimeters per minute (sccm) C_2H_4 and 900 sccm He-contained small water vapor from a tube furnace at atmospheric pressure. In the case of a water top-flow growth, only water vapor was introduced from a gas shower system placed above and parallel to the sample with 6−10 mm distance, and 100 sccm C_2H_4 and 900 sccm He gases flowed from tube furnace. C_2H_4 (10 sccm) and 90 sccm He with a controlled amount of water vapor was introduced from gas shower system for top-flow growth. The flowchart of the process is presented in Supporting Information, Figure S5). All furnaces were equipped with an *in situ* telecentric height monitoring system for growth kinetics measurement. TEM and Raman characterization showed that the CNTs were dominantly SWNTs.

Acknowledgment. Support from the Nanotechnology Program "Carbon Nanotube Capacitor Development Project" (2006-2011), by the New Energy and Industrial Technology Development Organization ("NEDO") is acknowledged.

Supporting Information Available: Photographs of experimental setup. This material is available free of charge *via* the Internet at http://pubs.acs.org.

REFERENCES AND NOTES

1. Maruyama, S.; Kojima, R.; Miyauchi, Y.; Chiashi, S.; Kohno, M. Low-Temperature Synthesis of High-Purity Single-Walled Carbon Nanotubes from Alcohol. *Chem. Phys. Lett.* **2002**, *360*, 229–234.
2. Hata, K.; Futaba, D. N.; Mizuno, K.; Namai, T.; Yumura, M.; Iijima, S. Water-Assisted Highly Efficient Synthesis of Impurity-Free Single-Walled Carbon Nanotubes. *Science* **2004**, *306*, 1362–1364.
3. Yamada, T.; Namai, T.; Hata, K.; Futaba, D. N.; Mizuno, K.; Fan, J.; Yudasaka, M.; Yumura, M.; Iijima, S. Size-Selective Growth of Double-Walled Carbon Nanotube Forests from Engineered Iron Catalysts. *Nat. Nanotechnol.* **2006**, *1*, 131–136.
4. Cantoro, M.; Hofmann, S.; Pisana, S.; Scardaci, V.; Parvez, A.; Ducati, C.; Ferrari, A. C.; Blackburn, A. M.; Wang, K.-Y.; Robertson, J. Catalytic Chemical Vapor Deposition of Single-Wall Carbon Nanotubes at Low Temperatures. *Nano Lett.* **2006**, *6*, 1107–1112.
5. Kayastha, V. K.; Wu, S.; Moscatello, J.; Yap, Y. K. Synthesis of Vertically Aligned Single- and Double-Walled Carbon Nanotubes without Etching Agents. *J. Phys. Chem. C* **2007**, *111*, 10158–10161.
6. Iwasaki, T.; Robertson, J.; Kawarada, H. Mechanism Analysis of Interrupted Growth of Single-Walled Carbon Nanotube Arrays. *Nano Lett.* **2008**, *8*, 886–890.
7. Zhao, B.; Futaba, D. N.; Yasuda, S.; Akoshima, M.; Yamada, T.; Hata, H. Exploring Advantages of Diverse Carbon Nanotube Forests with Tailored Structures Synthesized by Supergrowth from Engineered Catalysts. *ACS Nano* **2009**, *3*, 108–114.
8. Terrones, M.; Grobert, N.; Olivares, J.; Zhang, J. P.; Terrones, H.; Kordatos, K.; Hsu, W. K.; Hare, J. P.; Townsend, P. D.; Prassides, K.; Cheetham, A. K.; Kroto, H. W.; Walton, D. R. M. Controlled Production of Aligned-Nanotube Bundles. *Nature* **1997**, *388*, 52–55.
9. Fan, S.; Chapline, M. G.; Franklin, N. R.; Tombler, T. W.; Cassell, A. M.; Dai, H. Self-Oriented Regular Arrays of Carbon Nanotubes and their Field Emission Properties. *Science* **1999**, *283*, 512–514.
10. Wei, B. Q.; Vajtai, R.; Jung, Y.; Ward, J.; Hang, R.; Ramanath, G.; Ajayan, P. M. Organized Assembly of Carbon Nanotubes. *Nature* **2002**, *416*, 495–496.
11. Hofmann, S.; Ducati, C.; Kleinsorge, B.; Robertson, J. Direct Growth of Aligned Carbon Nanotube Field Emitter Arrays onto Plastic Substrates. *Appl. Phys. Lett.* **2003**, *83*, 4661–4663.
12. Jeong, H. J.; Kim, K. K.; Jeong, S. Y.; Park, M. H.; Yang, C. W.; Lee, Y. H. High-Yield Catalytic Synthesis of Thin Multiwalled Carbon Nanotubes. *J. Phys. Chem. B* **2004**, *108*, 17695–17698.
13. Eres, G.; Puretzky, A. A.; Geohegan, D. B.; Cui, H. *In Situ* Control of the Catalyst Efficiency in Chemical Vapor Deposition of Vertically Aligned Carbon Nanotubes on Predeposited Metal Catalyst Films. *Appl. Phys. Lett.* **2004**, *84*, 1759–1761.
14. Liu, J.; Czerw, R.; Carroll, D. L. Large-Scale Synthesis of Highly Aligned Nitrogen Doped Carbon Nanotubes by Injection Chemical Vapor Deposition Methods. *J. Mater. Res.* **2005**, *20*, 538–543.
15. Hart, A. J.; Laake, L. V.; Slocum, A. H. Desktop Growth of Carbon Nanotube Monoliths with *In Situ* Optical Imaging. *Small* **2007**, *5*, 772–777.
16. Pint, C. L.; Pheasant, S. T.; Pasquali, M.; Coulter, K. E.; Schmidt, H. K.; Hauge, R. H. Synthesis of High Aspect-Ratio Carbon Nanotube "Flying Carpets" From Nanostructured Flake Substrates. *Nano Lett.* **2008**, *7*, 1879–1883.
17. Hayamizu, Y.; Yamada, T.; Mizuno, K.; Davis, R. C.; Futaba, D. N.; Yumura, M.; Hata, K. Integrated Three-Dimensional Microelectromechanical Devices from Processable Carbon Nanotube Wafers. *Nat. Nanotechnol.* **2008**, *3*, 289–294.
18. Sekitani, T.; Noguchi, Y.; Hata, K.; Fukushima, T.; Aida, T.; Someya, T. A Rubber-like Stretchable Active Matrix Using Elastic Conductors. *Science* **2008**, *321*, 1468–1472.
19. Futaba, D. N.; Hata, K.; Yamada, T.; Hiraoka, T.; Hayamizu, Y.; Kakudate, Y.; Tanaike, O.; Hatori, H.; Yumura, M.; Iijima, S. Shape-Engineerable and High-Densely Packed Single-Walled Carbon Nanotubes. *Nat. Mater.* **2006**, *5*, 987–994.
20. Kong, J.; Franklin, N. R.; Zhou, C.; Chapline, M. G.; Peng, S.; Cho, K.; Dai, H. Nanotube Molecular Wires as Chemical Sensors. *Science* **2000**, *287*, 622–625.
21. Hiraoka, T.; Yamada, T.; Hata, K.; Futaba, D. N.; Kurachi, H.; Uemura, S.; Yumura, M.; Iijima, S. Synthesis of Single- and Double-Walled Carbon Nanotube Forests on Conducting Metal Foils. *J. Am. Chem. Soc.* **2006**, *128*, 13338–13339.
22. Lau, K. K. S.; Bico, J.; Teo, K. B. K.; Chhowalla, M.; Amaratunga, G. A. J.; Milne, W. I.; Mckinley, G. H.; Gleason, K. K. Superhydrophobic Carbon Nanotube Forests. *Nano Lett.* **2003**, *3*, 1701–1705.
23. Mukai, K.; Asaka, K.; Sugino, T.; Kiyohara, K.; Takeuchi, I.; Terasawa, N.; Futaba, D. N.; Hata, K.; Fukushima, T.; Aida, T. Highly Conductive Sheets from Millimeter-Long Single-Walled Carbon Nanotubes and Ionic Liquids: Application to Fast-Moving, Low-Voltage Electromechanical Actuators Operable in Air. *Adv. Mater.* **2009**, *21*, 1582–1585.
24. Zhang, M.; Fang, S.; Zakhidov, A. A.; Lee, S. B.; Aliev, A. E.; Williams, C. D.; Atkinson, K. R.; Baughman, R. H. Strong, Transparent, Multifunctional, Carbon Nanotube Sheets. *Science* **2005**, *309*, 1215–1219.
25. Qu, L.; Dai, L.; Stone, M.; Xia, Z.; Wang, Z. L. Carbon Nanotube Arrays with Strong Shear Binding-on and Easy Normal Lifting-off. *Science* **2008**, *322*, 238–242.
26. Gong, K.; Du, F.; Xia, Z.; Durstock, M.; Dai, L. Nitrogen-Doped Carbon Nanotube Arrays with High Electrocatalytic Activity for Oxygen Reduction. *Science* **2009**, *323*, 760–764.
27. Hafner, J. H.; Bronikowski, M. J.; Azamian, B. R.; Nikolaev, P.; Rinzler, A. G.; Colbert, D. T.; Smith, K. A.; Smalley, R. E. Catalytic Growth of Single-Wall Carbon Nanotubes from Metal Particles. *Chem. Phys. Lett.* **1998**, *296*, 195–202.

28. Yamada, T.; Maigne, A.; Yudasaka, M.; Mizuno, K.; Futaba, D. N.; Yumura, M.; Iijima, S.; Hata, K. Revealing the Secret of Water-Assisted Carbon Nanotube Synthesis by Microscopic Observation of the Interaction of Water on the Catalysts. *Nano Lett.* **2008**, *8*, 4288–4292.
29. Zhong, G.; Iwasaki, T.; Robertson, J.; Kawarada, H. Growth Kinetics of 0.5 cm Vertically Aligned Single-Walled Carbon Nanotubes. *J. Phys. Chem. B* **2007**, *111*, 1907–1910.
30. Ledermann, A.; Weber, U.; Mukherjee, C.; Schroeder, B. Influence of Gas Supply and Filament Geometry on the Large-Area Deposition of Amorphous Silicon by Hot-Wire CVD. *Thin Solid Films* **2001**, *395*, 61–65.
31. Andrea, P.; Schoder, B.; Bart, H.-J. Monte Carlo Simulations on Large-Area Deposition of Amorphous Silicon by Hot-Wire CVD. *Thin Solid Films* **2003**, *430*, 73–77.
32. Futaba, Don N.; Hata, K.; Namai, T.; Yamada, T.; Mizuno, K.; Hayamizu, Y.; Yumura, M.; Iijima, S. 84% Catalyst Activity of Water Assisted Growth, Single Walled Carbon Nanotube Forest Characterization by a Statistical and Macroscopic Approach *J. Phys. Chem. B* **2006**, *110*, 8035–8038.
33. Yasuda, S.; Futaba, D. N.; Yumura, M.; Iijima, S.; Hata, K. Diagnostics and Growth Control of Single-Walled Carbon Nanotube Forests using a Telecentric Optical System for In-situ Height Monitoring. *Appl. Phys. Lett.* **2008**, *93*, 143115-1–143115-3.
34. Futaba, D. N.; Hata, K.; Yamada, T.; Mizuno, K.; Yumura, M.; Iijima, S. Kinetics of Water-Assisted Single-Walled Carbon Nanotube Synthesis Revealed by a Time-Evolution Analysis. *Phys. Rev. Lett.* **2005**, *95*, 056104-1–056104-4.
35. Eres, G.; Kinkhabwala, A. A.; Cui, H.; Geohegan, D. B.; Puretkzy, A. A.; Lowndes, D. H. Molecular Beam-Controlled Nucleation and Growth of Vertically Aligned Single-Wall Carbon Nanotube Arrays. *J. Phys. Chem. B* **2005**, *109*, 16684–16694.
36. Iwasaki, T.; Robertson, J.; Kawarada, H. Mechanism Analysis of Interrupted Growth of Single-Walled Carbon Nanotube Arrays. *Nano Lett.* **2008**, *8*, 886–890.
37. Stadermann, M.; Sherlock, S. P.; In, J.-B.; Fornasiero, F.; Park, H. G.; Artyukhin, A. B.; Wang, Y.; Yoreo, J. J. D.; Grigoropoulos, C. P.; Bakajin, O.; Chernov, A. A.; Noy, A. Mechanism and Kinetics of Growth Termination in Controlled Chemical Vapor Deposition Growth of Multiwall Carbon Nanotube Arrays. *Nano Lett.* **2009**, *9*, 738–744.
38. Mizuno, K.; Ishii, J.; Kishida, H.; Hayamizu, Y.; Yasuda, S.; Futaba, D. N.; Yumura, M.; Hata, H. A Black Body Absorber from Vertically Aligned Single Walled Carbon Nanotubes. *Proc. Natl. Acad. Sci. U.S.A.* **2009**, *106*, 6044–6047.